ANALYSIS OF TRANSIENT SUPERSONIC HYDROGEN RELEASE, DISPERSION AND COMBUSTION

Breitung, W., Halmer, G., Kuznetsov, M. and Xiao, J.*

Institute of Nuclear and Energy Technologies,
Karlsruhe Institute of Technology (KIT)
Hermann-von-Helmholtz-Platz 1,
76344 Eggenstein-Leopoldshafen, Germany
***email: jianjun.xiao@kit.edu**

ABSTRACT

A hydrogen leak from a facility, which uses highly compressed hydrogen gas (714 bar, 800 K) during operation was studied. The investigated scenario involves supersonic hydrogen release from a 10 cm^2 leak of the pressurized reservoir, turbulent hydrogen dispersion in the facility room, followed by an accidental ignition and burn-out of the resulting H_2-air cloud. The objective is to investigate the maximum possible flame velocity and overpressure in the facility room in case of a worst-case ignition. The pressure loads are needed for the structural analysis of the building wall response. The first two phases, namely unsteady supersonic release and subsequent turbulent hydrogen dispersion are simulated with GASFLOW-MPI. This is a well validated parallel, all-speed CFD code which solves the compressible Navier-Stokes equations and can model a broad range of flow Mach numbers. Details of the shock structures are resolved for the under-expanded supersonic jet and the sonic-subsonic transition in the release. The turbulent dispersion phase is simulated by LES. The evolution of the highly transient burnable H2-air mixture in the room in terms of burnable mass, volume, and average H2-concentration is evaluated with special sub-routines. For five different points in time the maximum turbulent flame speed and resulting overpressures are computed, using four published turbulent burning velocity correlations. The largest turbulent flame speed and overpressure is predicted for an early ignition event resulting in 35 -71 m/s, and 0.13 – 0.27 bar, respectively.

Keywords: CFD, LES, hydrogen, dispersion, turbulent combustion, GASFLOW-MPI

1. Introduction and Objectives

The dispersion and combustion physics of hydrogen is influenced by many parameters. Depending on the detailed sequence of events, the damage potential of a hydrogen related accident can vary by orders of magnitude. The governing variables are released hydrogen mass, volume and average hydrogen concentration of the resulting H2-air cloud, ignition time and ignition location of the burnable H2-air cloud, the maximum flame speed developing for the given geometry, mixture properties, mixture confinement and scale, and the resulting maximum overpressure. For the possible combustion regimes of slow laminar deflagration, fast turbulent deflagration, and fully developed detonation, typical flame speeds and resulting unreflected overpressures roughly vary by three orders of magnitude (2 – 2000 m/s, 0.01 – 10 bar). Therefore, a realistic evaluation of the damage potential of a given accident scenario requires mechanistic modeling of the chain of physical events with modern 3-D numerical tools. Such a systematic and self-consistent methodology was developed at KIT and presented earlier to the ICHS hydrogen safety community [1].

The main challenge for numerical simulation of hydrogen dispersion and combustion scenarios in real scale industrial facilities is the fact, that a wide range of time, space, and flow velocity scales must be

resolved. A new CFD program, called GASFLOW-MPI, was specifically developed at KIT to model this class of challenging coupled inert/reactive flow problems [2].

In the accident scenario analyzed in this paper, the time scale ranges from 10^{-6} to 10^{0} s, the length scale from 10^{-3} to 10^{1} m, and the flow velocity from 10^{0} to 10^{3} m/s. GASFLOW-MPI is well suited to model this problem because it allows to use a) massive parallel programming, b) semi-implicit solvers validated for broad flow velocities of interest (M = 0.001 to 5), c) robust second order schemes for convection terms, d) different turbulence models, e) non-equidistant Cartesian or cylindrical grids, and f) special routines for risk evaluation of the computed inhomogeneous and time-dependent hydrogen-air mixtures. The accident scenario described in this paper requires application of all these numerical simulation capabilities.

The objectives of the 3-D numerical simulation are: (1) simulate the unsteady supersonic flow from the high pressure reservoir, (2) model the H2/air mixture evolution in the facility room, (3) calculate the main risk parameters like mass, volume, and average hydrogen concentration of the transient burnable H2-air cloud, and (4) provide the necessary information for estimates of the maximum turbulent flame velocity. The maximum flame velocities and overpressures possible in this hydrogen release scenario were estimated by using different published turbulent burning relations. The obtained pressure loads serve as input to an analysis of the dynamic wall response.

The study is related to a particle accelerator which uses highly compressed hydrogen as driving fluid. Failure of a facility component is assumed at a time during the compression process at which the hydrogen self-ignition temperature is not yet reached. In this case a burnable H2-air mixture would develop in the facility room, which after an accidental late ignition, could result in significant pressure loads to the walls. A mechanical failure later in the compression process, at which the hydrogen gas has been heated above the self-ignition temperature, would result in a self-ignited burning jet with much less pressure development. The conservative case of a late ignition is investigated here.

2. Problem Geometry, Initial Conditions, Hydrogen Equation-of-state and Computational Grid

The scenario investigates a postulated hydrogen release from a particle accelerator which is located in a room 21 m long, 4 m wide and 2.5 m high. Since the hydrogen leak is positioned in the center of the room, two vertical symmetry planes exist, and only one quarter of the room needs to be modeled, resulting in a computational domain of 10.5m x 2m x 2.5m = 52.5 m^3.

Hydrogen is released from a small high pressure reservoir having the following initial conditions: T_0 = 800 K (which is below the self-ignition temperature), p_0 = 714 bar, $V_0 = 2.6\ 10^{-4}$ m^3 (260 cm^3), H_2 mass in the reservoir $5.63*10^{-3}$ kg, release area 10 cm^2, release direction vertically upwards. The high pressure reservoir is 207.28 mm long, 35.45 mm wide, and 35.45 mm high. The leak area is located in the upper surface of the rectangular reservoir, having the dimensions 3.1623 cm x 3.1623 cm = 10 cm^2. The facility room is initially filled with air at 1 bar and 298.15 K. Room walls are also at 298.15 K, they are modeled adiabatically with a no-slip boundary condition.

The initial hydrogen density in the reservoir is 21.5 kg/m^3. Despite of this high density, hydrogen may be modeled as ideal gas because, due to the relatively high initial temperature T_0, the compressibility factor Z in the reservoir is 1.06, hence close to ideal gas behavior. Also the strong cooling of the hydrogen during the supersonic expansion process from the reservoir into the low pressure environment causes no significant non-ideality because of the rapidly decreasing pressure.

Using the default GASFLOW mesh generator a Cartesian, non-equidistant mesh was constructed to discretize the x-, y-, and z-axes in a suitable way. The mesh size increases with increasing distance from the source region. The number of numerical cells in x, y, and z direction is 220, 140, and 250, respectively, resulting in totally 7.7 million cells. The smallest cell size of 0.079 cm is used in the reservoir region. The break area was resolved in the numerical model (= 1/4 of 10 cm^2 total area) with 20 x 20 = 400 cells. The GASFLOW capability to define non-equidistant grids is an important

prerequisite for simulating the present problem of a very small high pressure reservoir in a large room. The room-to-reservoir volume ratio is about 10^6. Fig. 1 depicts the mesh in the x-z and the y-z plane, together with a density plot obtained 1 ms after begin of the release. Since the hydrogen release is in upward direction, a denser grid is applied in the upper half of the computational domain (z>0).

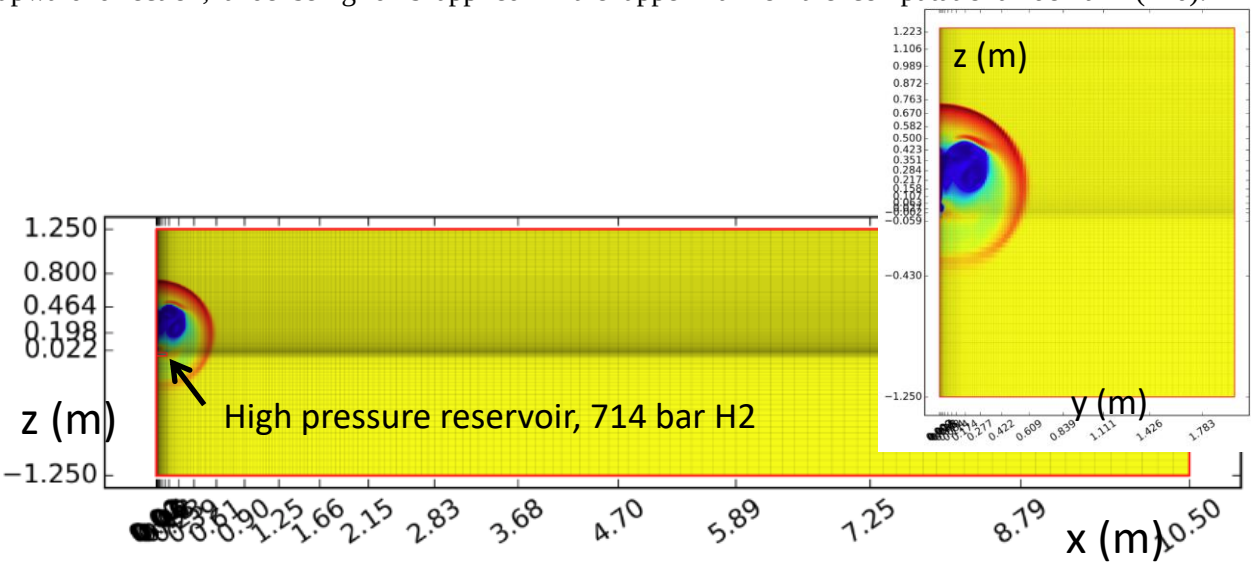

Figure 1. Non-equidistant 3-D grid used in the GASFLOW-MPI simulation. The smallest cell size of 0.79 mm is used near the high pressure reservoir, total number of cells is 7.7 million.

3. High Pressure Hydrogen Release and Hydrogen Dispersion in the Facility Room

The release of hydrogen from a small high pressure reservoir into a large room at ambient conditions is a complex process involving different flow phenomena like supersonic flow, transition to sub-sonic flow, momentum dominated jet, buoyancy dominated plume, and flow interactions with the enclosing walls. This chapter describes the sequence of hydrogen release phenomena in two steps: first, the early rapid expansion process from the reservoir, and secondly, the slower subsequent hydrogen dispersion in the room.

The blow-down of hydrogen gas from a high-pressure reservoir through a small leak was modeled in [3]. The used methodology including real-gas behavior leads to the mass fluxes shown in Fig. 2 for three different initial reservoir pressures. The dimensionless time t^+ and mass flux G^+ are defined as $t^+ = t/t_{char}$ with $t_{char} = V/(A \cdot c_r)$, and $G^+ = G/G_{char}$ with $G_{char} = \rho_r \cdot c_r$. Here V is the reservoir volume, A is the break area, ρ_r is the initial hydrogen density, and c_r is the initial sound speed in the reservoir. The stars represent the times where the pressure ratio between reservoir and ambient pressure falls below 1.9 and the flow velocity in the throat changes from sonic to subsonic. For the initial reservoir conditions in the present problem t_{char} becomes 0.12 ms. Therefore results for three different times are discussed now, representing the fully developed under-expanded jet (t= 0.6 ms, t^+=5), a time characteristic for the sonic-subsonic transition (t=1 ms, t^+=8.3), and a time for the subsonic flow regime (t=3ms, t^+=25).

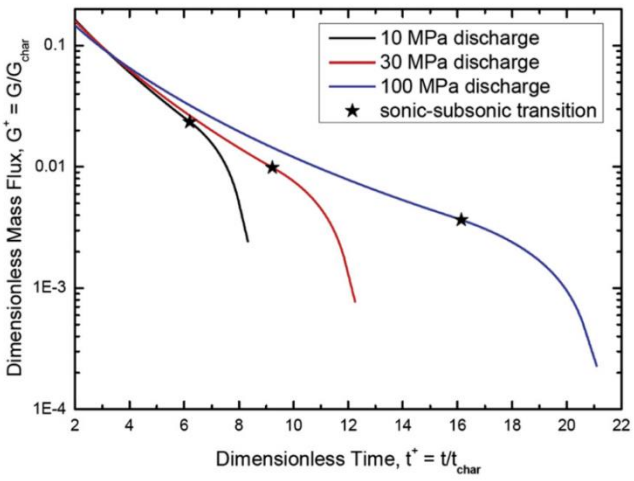

Figure 2. Calculated dimensionless hydrogen mass flux from a high pressure hydrogen gas reservoir [3]. The initial pressure in the present problem is 71.4 MPa.

Figures 3a and 3b depict calculated flow variables for the fully developed under-expanded supersonic jet, 0.6 ms after begin of the hydrogen release. In the left part of Fig. 3a the velocity magnitude is shown, the walls of the reservoir are indicated in red. The velocity field shows the typical barrel shock and Mach disc structures. Gas which passes through the Mach disc is slowed down to M<1, whereas gas which passes through the barrel shock, remains supersonic. The barrel region, with supersonic velocities of up to 2800 m/s, is about 16 cm long and 14 cm wide (y= 0 is a symmetry plane). Due to the very high reservoir-to-ambient pressure ratio of 71.4 / 0.1, the gas expansion causes the hydrogen to leave the reservoir in vertical and almost horizontal direction. Therefore hydrogen expands nearly the same distances in vertical and horizontal directions, as visible in the hydrogen volume fraction plot (right side of Fig. 3a). The volume fraction scale ranges from 0 to 4 vol%; brown color indicates hydrogen volume fractions above 4 %. Only a very thin mixing layer with air exists at this time.

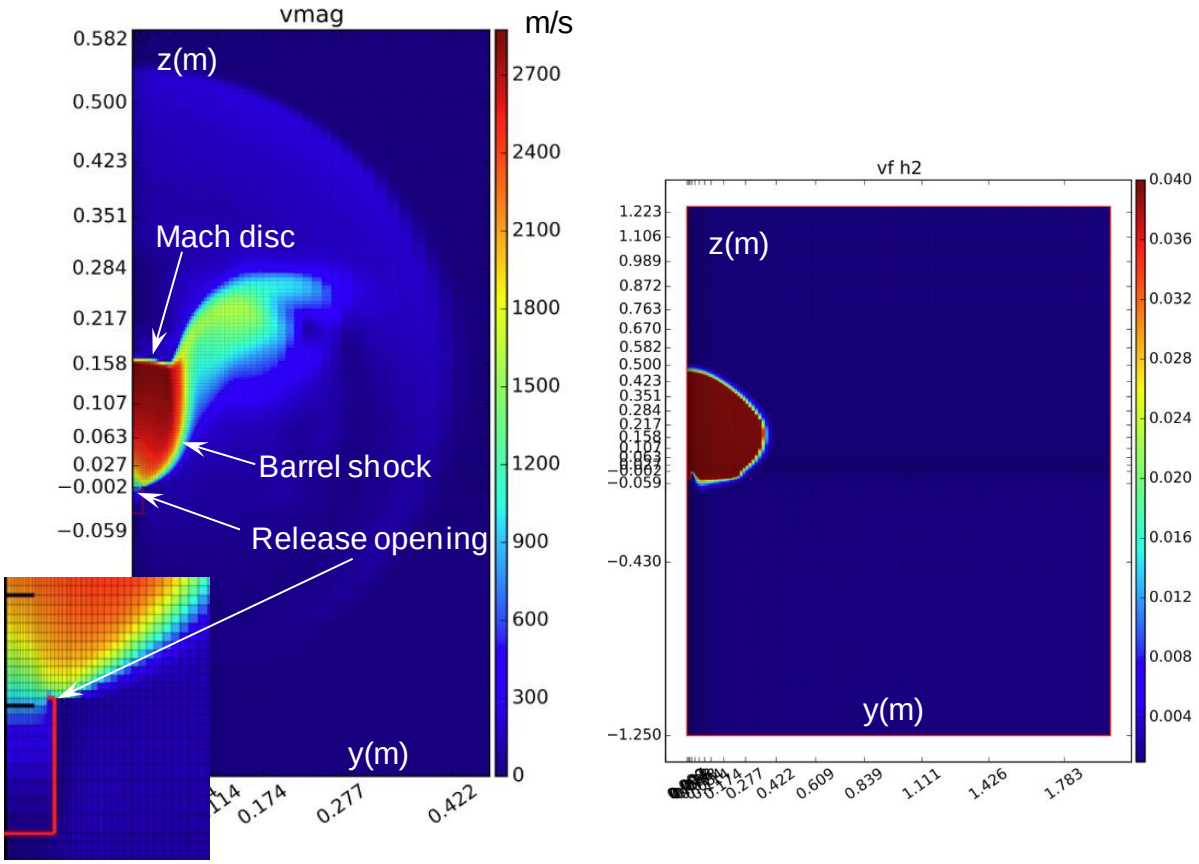

Figure 3a. Flow variables for fully developed under-expanded supersonic jet **0.6 ms** after begin of hydrogen release (vmag = velocity magnitude in m/s, vfh2 = hydrogen volume fraction)

The density plot in Fig. 3b below shows that an asymmetric spherical pressure wave is emitted from the Mach disc position - not the release opening - with air densities of up to about 2 kg/m^3. The regions with high hydrogen concentrations (in blue) have much lower gas densities, compared to the surrounding air. The temperature distribution is very different at this time (right side of Fig. 3b) ranging from 80 K in the barrel structure to 400 K in the pressure wave front moving upwards.

Figure 4 depicts the velocity and hydrogen volume fraction at 1 ms, which is close to the sonic-subsonic transition. The sonic jet has almost completely collapsed due to the pressure decay in the hydrogen reservoir, as can be seen in the magnified insert. The maximum velocity has decreased to about 1800 m/s and only a small part of the earlier barrel region remains at this time. A very narrow cone of high velocity gas extends up to about 25 cm from the release opening. The hydrogen cloud has expanded about 54 cm vertically and 42 cm in y-direction. The corresponding oxygen field shows that at this time most of the hydrogen is not burnable due to insufficient oxygen content (< 5 vol% O_2).

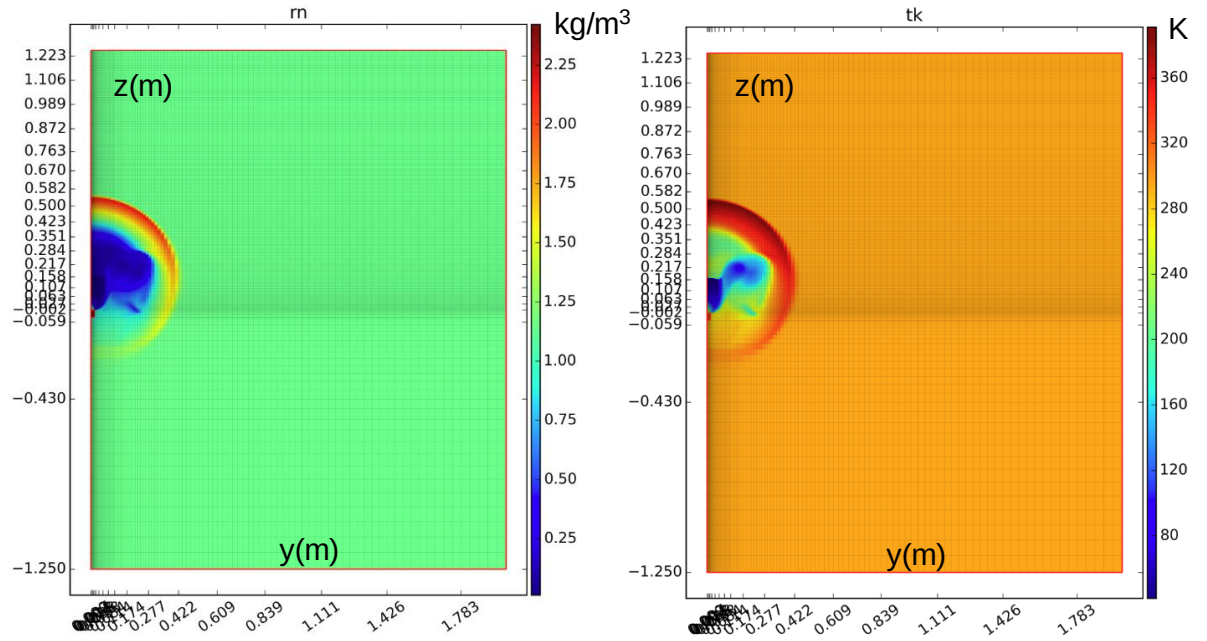

Figure 3b. Flow variables for fully developed under-expanded supersonic jet **0.6 ms** after begin of hydrogen release (rn = density in kg/m^3), tk = temperature in K)

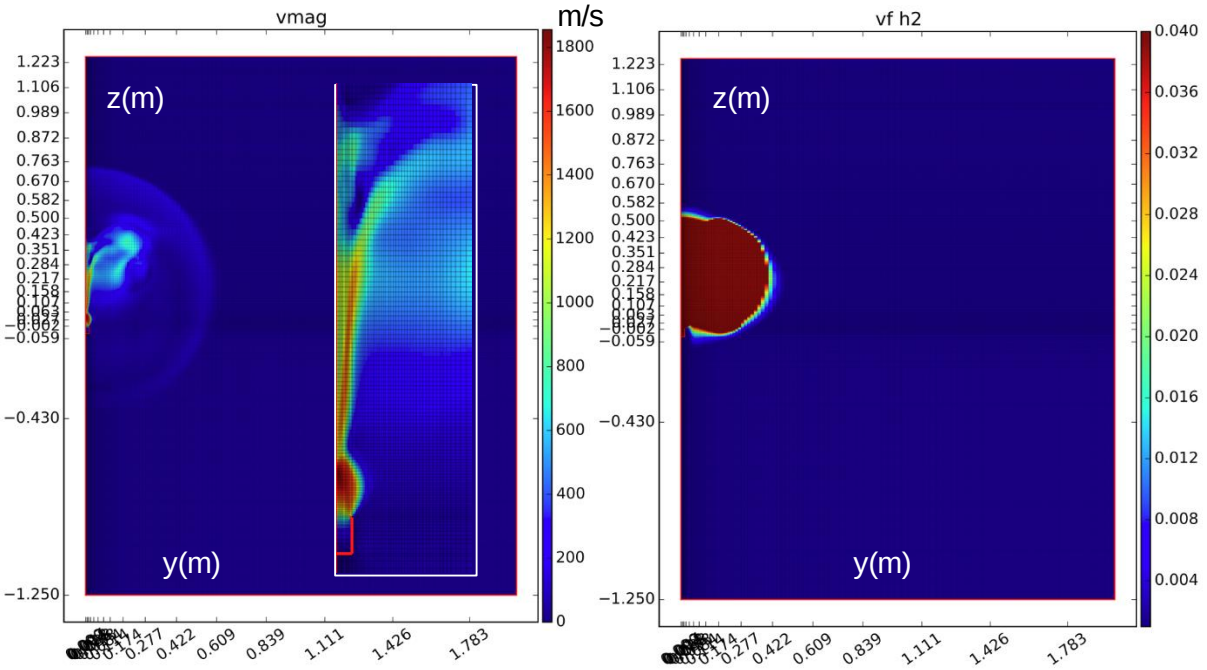

Figure 4. Flow variables for the sonic-subsonic transition, **1 ms** after begin of hydrogen release (vmag = velocity magnitude in m/s, vfh2 = hydrogen volume fraction).

Figure 5 shows the same variables for a time in which the flow has become subsonic (at 3 ms). The velocity magnitude has further decreased to less than 500 m/s. A reflected wave is returning from the ceiling of the room. The hydrogen cloud has now detached from the reservoir opening and is moving preferentially upwards to the ceiling as a momentum dominated jet. The expansion in y-direction is still close to 42 cm. The corresponding oxygen concentration plot shows that already at this time, turbulent mixing with air has led to a burnable H_2-air mixture in most of the hydrogen cloud (> 5 vol% O2). The addition of warm air has increased the cloud temperature to the range of 200 – 250 K.

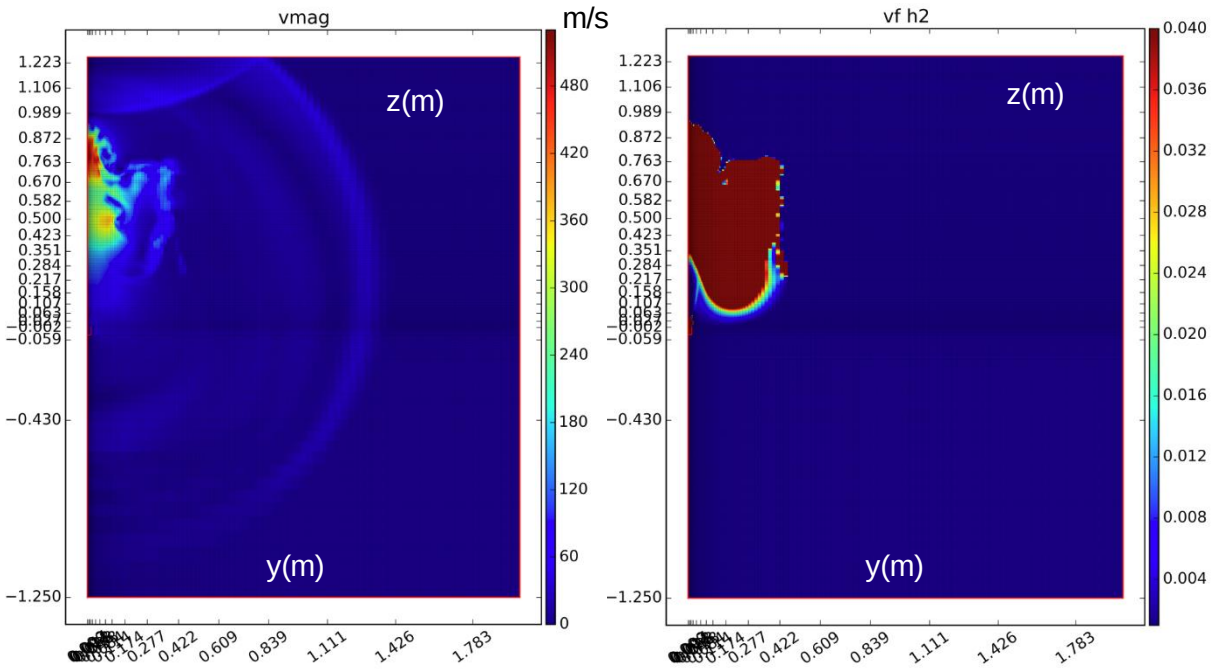

Figure 5. Flow variables for jet near the sonic-subsonic transition, **3 ms** after begin of hydrogen release (vmag = velocity magnitude in m/s, vfh2 = hydrogen volume fraction).

The hydrogen jet shown in Figure 5, reaches the ceiling of the room about 8 ms after begin of the release. Figure 6 shows flow velocity magnitudes and hydrogen volume fractions at a point in time where the vertical flow has been re-directed by the ceiling into the horizontal direction (90 ms). The buoyancy dominated plume has already travelled about 1.2 m towards the side wall, which is located

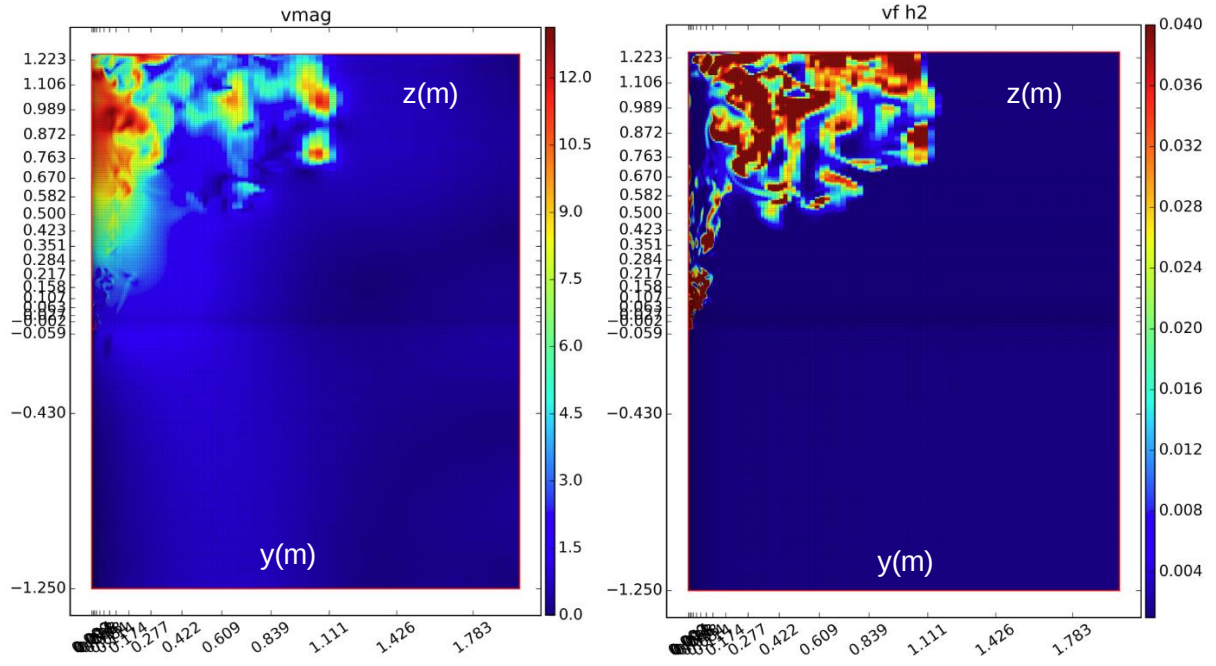

Figure 6. Flow variables for the buoyancy dominated plume moving horizontally underneath the ceiling of the room, **90 ms** after begin of hydrogen release (vmag = velocity magnitude in m/s, vfh2 = hydrogen volume fraction)

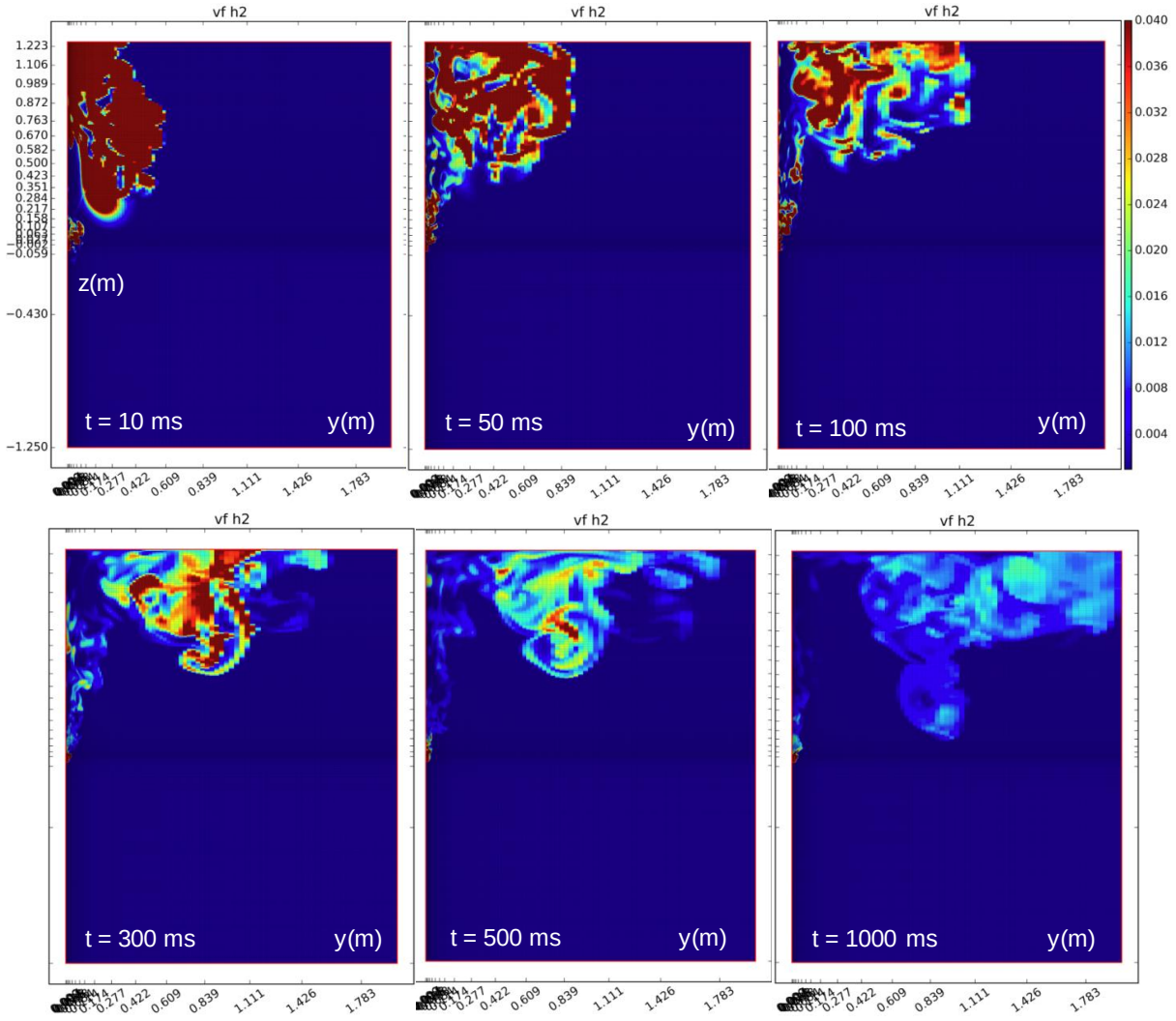

Figure 7. Development of hydrogen dispersion in the facility room after release from the high pressure reservoir. Shown are hydrogen volume fractions in the y-z plane (0-4 vol%). Brown regions contain burnable H2-air mixtures with more than 4 vol% hydrogen.

at y= 2m. The velocity magnitude has further decreased to less than 15 m/s. The brown regions in the hydrogen volume fraction plot contain burnable mixtures because they have more than 4 vol% H_2 and 16 – 20 vol% O_2. In the remaining colored regions the turbulent mixing with air has diluted the hydrogen to unburnable concentrations below 4 vol% H_2. Although the hydrogen reservoir has been depressurized at this time, small amounts of hydrogen are still released from the reservoir, forming small regions with rising, burnable H_2-air mixtures.

An overview of the complete hydrogen dispersion process in the facility room is presented in Fig.7. At 10 ms a compact H2-air cloud moves rapidly upwards. The corresponding O_2-field shows that the cloud consists nearly completely of burnable mixtures, shown in brown color. With increasing time the cloud moves sideways, and turbulent admixture of air decreases the burnable volume continuously. After 1000 ms the cloud has reached the vertical side wall at y=2 m and begins a downward motion. The velocity magnitudes in the cloud have decreased to only 1 – 2 m/s. No burnable H_2-air mixtures are left in the room at this time. The largest hazard in this release scenario exists therefore early in time, when practically all of the released hydrogen inventory is in a fast burnable state.

GASFLOW-MPI contains subroutines which allow to evaluate the risk for different combustion regimes in case of an accidental ignition of the generated hydrogen-air cloud. At each point in time every

computational node in a specified computational sub-domain (called room) is analyzed with respect to its local hydrogen concentration and hydrogen mass, and global cloud properties are calculated from this information by summing over all nodes.

Fig. 8 (left) depicts the average hydrogen concentration in the burnable cloud, which has between 4 and 75 vol% H_2, as function of time. Room 2 refers to the upper half of the facility room (z > 0). Between 1 and 10 ms after begin of the release the average hydrogen concentration of the burnable cloud ranges from 31 to 38 vol%, which indicates quite reactive mixtures. Thereafter, turbulent mixing with air continuously dilutes the hydrogen gas. The concentration specific hydrogen masses give additional insight into the dilution process (right part of Fig.8). For each point in time the hydrogen mass is plotted which is above the six given concentration limits. The light blue line shows for instance the growth and decay of the hydrogen mass with hydrogen concentrations above 16 vol%, and the red line shows the evolution of the hydrogen mass above 4 vol%. Turbulent mixing transfers hydrogen from higher to lower concentrations. The data show that the highest burnable mass occurs around 10 ms; at this time practically the whole released hydrogen mass is in a burnable composition. The dark blue line depicts the total hydrogen inventory (with c_{H2}> 0 vol%) which amounts to 1.41 g for the quarter jet modeled here (m_{H2}= 5.63 g /4).

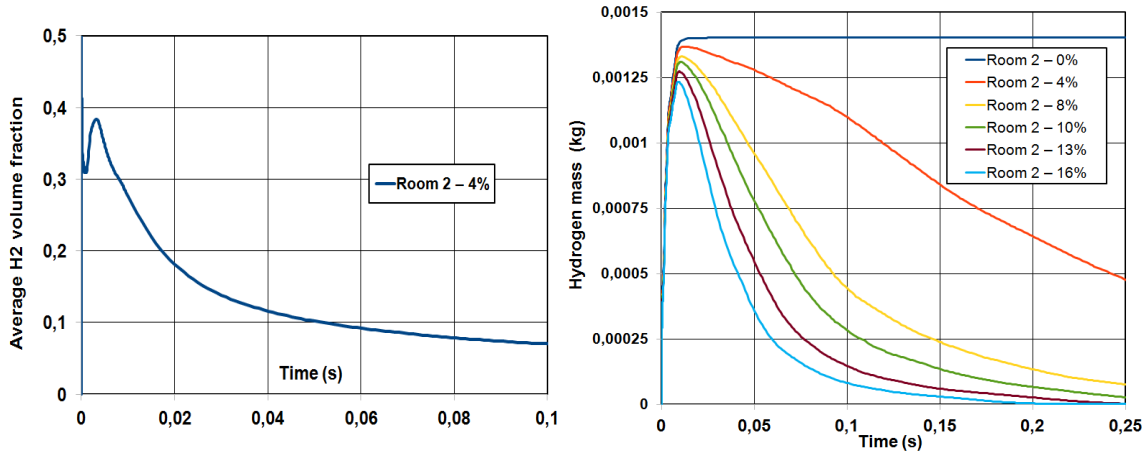

Figure 8. Development of the average hydrogen volume fraction in the burnable cloud during the dispersion process (left) and evolution of hydrogen masses within a cloud above a certain level of hydrogen concentration in the investigated release scenario (right).

To test the effect of the turbulence model on the dispersion process, the simulation was repeated with the k-ε and the algebraic default model (ALG) of GASFLOW-MPI. The standard k- ε model did not converge in this very dynamic flow problem. Comparing the LES and ALG turbulence models, the local flow variables show some differences, but the global properties of the burnable cloud, like shape, volume and average hydrogen concentration, agree surprisingly well. The data of Fig. 8 for the ALG and LES model show only minor differences. The transient hydrogen dispersion computed with LES seems to provide a reliable basis for estimating possible combustion processes in case of an accidental ignition.

An important question for risk evaluation is, if after the ignition, the flame can accelerate spontaneously to sonic velocities or even undergo a transition to detonation. GASFLOW-MPI evaluates the σ-criterion for flame acceleration [4] and the 7λ-criterion for deflagration-to-detonation transition [5] in each time step during the calculation. Both criteria were fulfilled at early times in the present release scenario, but since these criteria were derived for fully confined mixtures, and the H_2-air cloud in this problem was only partially confined by the ceiling, the possibility for sonic flames and detonation onset appears very remote. It is therefore sufficient to investigate which turbulent flame velocities can develop for the present mixture and turbulence conditions due to flame folding and instabilities.

4. Evaluation of Maximum Combustion Pressures

GASFLOW-MPI includes combustion subroutines to simulate the dynamics of turbulent flame propagation. To model the flame front propagation, the transport equation of the density-weighted mean reaction progress variable is solved. Arrhenius rate for chemistry and different turbulence models for combustion are implemented into the GASFLOW-MPI code [2]. Before running numerical simulations, a simplified method for evaluation of flame propagation regimes in hydrogen-air mixtures formed by high-pressure hydrogen release was developed, using different semi-empirical correlations. The method is based on exponential fits of dimensionless turbulent flame velocity S_T normalized by fundamental laminar burning velocity S_L against the major dimensionless characteristics, mixture reactivity and stability of the system:

$$\frac{S_T}{S_L} = F\left(\frac{u'}{S_L}, \frac{L}{\delta}, Le, Ze, ...\right) \quad (1$$

where u' is the level of turbulent fluctuations; L is the integral length scale; $\delta = \chi / S_L$ is the laminar flame thickness as a measure of chemical reactivity; χ is the thermodiffusivity of the mixture; *Le* and *Ze* are Lewis and Zeldovich numbers as measures of flame stability. Similar to [8], several semi-empirical correlations are chosen for practical applications to cover wider range of variables in equation (1). The Gülder formula [9]

$$\frac{S_T}{S_L} = 1 + 0.7\left(\frac{u'}{S_L}\right)^{3/4}\left(\frac{L}{\delta}\right)^{1/4} \quad (2$$

covers the range of relatively low turbulent Reynolds numbers *Re* < 3200. The other formulas of Bray [10], Bradley [11], and Shy [12] cover a wider range of turbulent Reynolds numbers from *Re* < 6000 to *Re* < 25000, which are typical for highly turbulent flames and larger scales:

$$\frac{S_T}{S_L} = 1.8\left(\frac{u'}{S_L}\right)^{0.412}\left(\frac{L}{\delta}\right)^{0.196} \quad (3$$

$$\frac{S_T}{S_L} = 1.53\left(\frac{u'}{S_L}\right)^{0.55}\left(\frac{L}{\delta}\right)^{0.15} Le^{0.3} \quad (4$$

$$\frac{S_T}{S_L} = 1 + 0.05\left(\frac{u'}{S_L}\right)^{0.39}\left(\frac{L}{\delta}\right)^{0.61} \quad (5$$

The advantage of equation (4) is that it takes into account the flame sensitivity to thermal diffusion instability. This is of great importance for the lean hydrogen-air mixtures appearing in dispersion scenarios of high pressure hydrogen jets into air (see Fig.8). After an ignition the hydrogen-air mixture within the flammability limits may burn and then accelerate depending on mixture reactivity, level of turbulence, dimensions and geometry of the system. Maximum combustion velocity and combustion overpressure govern the integral hazard of a combustion process. Of course, integral scale and total hydrogen inventory also influence the risk from a combustion process.

Figures 4-7 demonstrate the very high non-uniformity of hydrogen in the cloud. The characteristic size of the cloud grows with time, combined with a reduction of the hydrogen concentration. The amount of burnable hydrogen, after it reaches the maximum (~4 g at 10 ms, Fig. 8) reduces quicker with increasing average hydrogen concentration. The question is what is the governing property of the cloud leading to a high combustion velocity and pressure? Smaller volume of higher hydrogen concentration may lead to higher distant pressure compared to larger volume and lower concentration keeping the same amount of hydrogen. Fig. 9 shows that there is a maximum volume of burnable hydrogen-air mixture above the specified level of hydrogen concentration. For our analysis, we choose the ignition time delay

corresponding to the maximum volume of the mixture above different levels of hydrogen concentration (4, 8, 10, 13, and 16 vol% H_2). Table 1 contains the initial conditions corresponding to different combustion scenarios at different ignition time delays t_{max} to be used in equations (2)-(5). The integral length scale is assumed to be equal to maximum diameter of burnable cloud $L=2R_{max}$ above different level of hydrogen concentration C_{H2min}.

Table 1. Initial conditions for different combustion scenarios.

C_{H2min} (vol. %)	R_{max} (m)	t_{max} (s)	m_{H2} (g)	C_{av} (%H2)	S_L (m/s)	T_b K	σ (-)	u' (m/s)
4	0.56	0.100	4.020	6.65	0.043	834	2.75	1.97
8	0.44	0.042	4.144	14.4	0.36	1420	4.50	3.70
10	0.40	0.030	4.260	18.6	0.75	1727	5.34	4.74
13	0.37	0.024	4.084	23.6	1.35	2066	6.23	5.69
16	0.34	0.018	4.205	30.1	2.22	2390	7.02	10.5

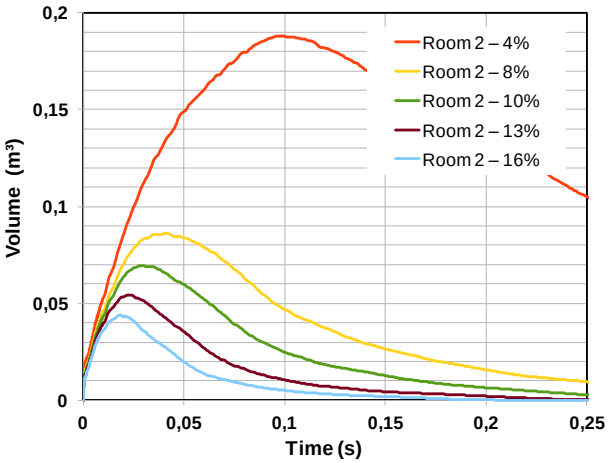

Figure 9. Evolution of burnable volumes during the dispersion and mixing process in the space above the release opening (called Room 2). The volumes are differentiated with respect to their minimum hydrogen concentration, red = > 4vol%, yellow = > 8 vol %, and so on. Ignitions are assumed at the times of maximum volume, e.g. at 0.10 s for the > 4 vol% cloud, and 0.42 s for the > 8 vol% cloud. The volumes shown in Fig. 9 relate to the simulated quarter jet.

For the different scenarios, the total amount of burnable hydrogen m_{H2} at different ignition times, corresponding to t_{max}, is almost the same in this early phase of the release (~4 g H2). This will be an advantage to properly compare combustion characteristics for different scenarios. The main thermodynamic and combustion properties (adiabatic combustion temperature T_b, laminar flame velocity S_L, and expansion ratio of combustion products σ) were calculated using the STANJAN and Cantera codes [13, 14]. The burnable hydrogen mass m_{H2}, average H2 concentration C_{av} and the turbulent fluctuation u' for all scenarios to be analyzed in Table 1 were extracted from GASFLOW-MPI simulations for different ignition moments, corresponding to maximum size of burnable cloud.

Turbulent burning velocities for the five different scenarios (Table 1) were calculated using the four relations of Eqs. (2) - (5). Figure 10 shows that the turbulent burning velocity quickly decreases from 80 m/s to 1-3 m/s with increasing ignition time from 18 to 100 ms. Considering the combustion process as a flow of combustion products, a pressure wave will be generated. The overpressure from such a pressure wave can be calculated, according to gasdynamics as:

$$p = p_0\left(1+\frac{\gamma-1}{2}\frac{v}{c_r}\right)^{\frac{2\gamma}{\gamma-1}} \qquad (6$$

where p_0 is the ambient pressure; v is the flow velocity, assumed to be equal to the turbulent flame velocity S_T, c_r is the speed of sound in hydrogen-air cloud, and γ is the adiabatic coefficient. Figure 11 shows that the maximum combustion pressure of 100-300 mbar, corresponding to the maximum turbulent flame speed of 60-80 m/s, reduces almost 100 times by changing the ignition delay for the hydrogen jet from 20 to 100 ms after opening of the vessel. Such a behavior is very close to our experimental data for ignition of high pressure hydrogen jets [15]. The measured maximum combustion overpressure from ignited hydrogen jets of about 150-200 mbar, occurred at ignition delay times in the range of 15-30 ms after opening of the pressurized vessel. The calculated combustion pressure in this study is considered as a relatively hazardous event which should be mitigated for safety reasons. The distant pressure outside of burnable cloud can be evaluated for gaseous explosion using dimensionless Sachs coordinates [16].

The simplified method used to evaluate the hazard of a hydrogen cloud explosion, demonstrated very good agreement with experimental results [15]. The next step will be numerical GASFLOW-MPI simulations of the combustion processes, which we may then compare to the simplified method.

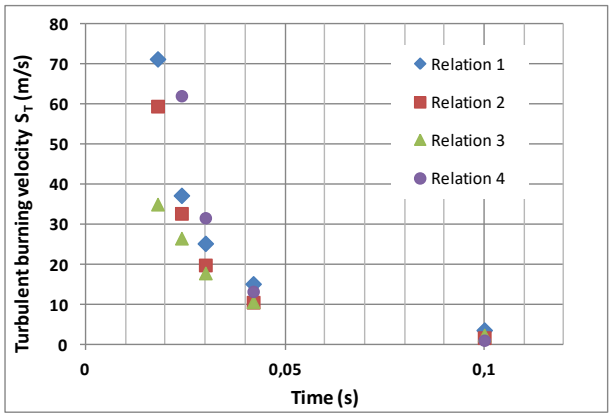

Figure 10. Calculated turbulent burning velocities for five different ignition times during the hydrogen dispersion process, using the S_T-correlations from Equations (2) - (5)

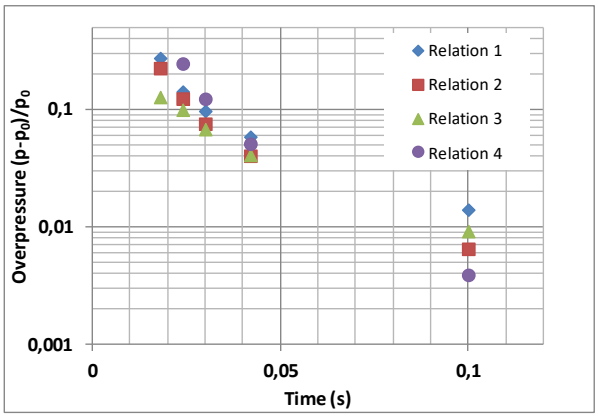

Figure 11. Calculated overpressures for five different ignition times during the hydrogen dispersion process

5. Conclusions

A hydrogen leak from a facility, which uses highly compressed hydrogen gas during operation was studied. The investigated accident scenario involves supersonic hydrogen release from a 10 cm^2 leak of the pressurized reservoir (initially at 714 bar, 800 K), turbulent hydrogen dispersion and mixing with air in the facility room, followed by an accidental ignition and burn-out of the resulting H_2-air cloud. This complex flow problem, which deals with a wide range of length scales (10^{-3} – 10^{1} m), time scales (10^{-6} – 10^{0} s), and flow velocities (10^{0} – $3\cdot10^{3}$ m/s) was simulated with all-speed CFD code GASFLOW-MPI. The main phases of the supersonic and sub-sonic hydrogen release from the reservoir, as well as the subsequent turbulent dispersion were simulated. Using specially developed GASFLOW routines the risk parameters of the resulting time-dependent H_2-air mixture were computed. The largest amount of burnable H_2-mass exists already 10 ms after begin of the release. At this time practically the whole H_2-inventory is in a highly reactive state with mean H_2-concentrations from about 30 - 40 vol %, a volume of about 0.250 m^3, and a very high turbulence level. Due to the adiabatic expansion process the H_2-air mixture is cold (240 – 280 K), increasing the energy density of the burnable mixture. The continuous turbulent mixing of air into the H_2-air cloud due to the velocity gradients, leads to a fast dilution of the

released hydrogen; after 0.5 s nearly no burnable hydrogen is left. A validated LES turbulence model was used to predict the very dynamic H_2-dilution process. A summary of the systematic and very extensive validation work performed for the GASFLOW code is given in Chapter 6 of [17], more recent examples are presented in [2].

The turbulent flame velocities, S_T, for the transient H_2-air mixtures were estimated with a simplified method using four different models for five different ignition times. The highest turbulent flame velocities were obtained for an early ignition (at 18 ms) resulting in $S_T = 35 – 71$ m/s. According to gas dynamics, such a flame speed leads to overpressures in the range of 0.13 to 0.27 bar. An early ignition event is not unrealistic because the hydrogen cloud has reached the ceiling already 10 ms after begin of the H_2-release and fluorescent lamps may be installed at the ceiling. An upwards directed overpressures may be a challenge for civil buildings because these are normally designed for downwards directed gravity forces. Combustion models in GASFLOW-MPI has been intensively developed and validated in the past years. GASFLOW-MPI simulations of H_2-air mixtures in the very dynamic flow will be performed soon.

References

1. Breitung, W., Analysis methodology for hydrogen behaviour in accident scenarios. International Conference on Hydrogen Safety, Pisa, Italy, 8-10 September 2005
2. Xiao, J., Travis, J.R., Royl, P., Necker, G., Svishchev, A., and Jordan, T., Three-dimensional all-speed CFD code for safety analysis of nuclear reactor containment: Status of GASFLOW parallelization, model development, validation and application, *Nuclear Engineering and Design* **301**, 2016, pp. 290-310
3. Xiao, J., Travis, J.R., Breitung, W., Hydrogen release from a high pressure gaseous hydrogen reservoir in case of a small leak, *Int. Journal of Hydrogen Energy* **36**, 2011, pp. 2545-2554
4. Dorofeev, S.B., Kuznetsov, M.S., Alekseev, V.I., Efimenko, A.A., and Breitung, W., Evaluation of limits for effective flame acceleration in hydrogen mixtures, Journal of Loss Prevention in the Process Industries, **14**, 2001, pp. 583-589
5. Dorofeev, S.B., Sidorov, V.P., Kuznetsov, M.S., Matsukov, I:D. and Alekseev, V.I., Effect of scale on the onset of detonations, *Shock Waves* **10**, 2000, pp. 137-149
6. Landau, L.D. and Lifshitz, E.M., Mechanics. (A Course of Theor. Physics), Pergamon Press 1969
7. Xiao, J., Travis, J. R., Kuznetsov, M., Numerical investigations of heat losses to confinement structures from hydrogen-air turbulent flames in ENACCEF facility, *International Journal of Hydrogen Energy*, **40**(38), 2015, pp. 13106-13120.
8. Dorofeev, S. B., A flame speed correlation for unconfined gaseous explosions. Proc. Safety Prog., **26**, 2007, pp. 140–149.
9. Gülder, O.L., Turbulent premixed combustion modelling using fractal geometry, *Proceedings of the Combustion Institute* **23**,1991, p. 835-842
10. Bray, K.N.C, Studies of Turbulent Burn.Veloc., *Proc. R. Soc. London. A* **431**, 1990, pp. 315- 335
11. Bradley, D., Gaskell, P.H., Gu, X.J., Burning velocities, Markstein lengths, and flame quenching for spherical methane-air flames: a computational study, *Combust. Flame* **104** ,1996, pp.176-198
12. Shy, S.S., Lin, W. J., Peng, K.Z., High intensity turbulent premixed combustion: general correlations of turbulent burning velocities in a new cruciform burner, *Proc. Combust. Inst*. **28**, 2000, pp. 561-568
13. Reynolds, W.C., The Element Potential Method for Chemical Equilibrium Analysis: Implementation in the Interactive Program STANJAN Version 3, Dept. of Mechanical Engineering, Stanford University, Palo Alto, California, January 1986.
14. Goodwin, D.G., Cantera User's Guide, Cal. Institute of Techn., Pasadena, CA, November, 2001.
15. Grune, J., Sempert, K., Kuznetsov, M., Breitung, W., Experimental study of ignited unsteady hydrogen jets into air, *International Journal of Hydrogen Energy*, **36(3)**, 2011, pp. 2497-2504.
16. Dorofeev, S.B., Sidorov V.P., Kuznetsov M.S., Dvoinishnikov A.E., Alekseev V.I., Efimenko A. Air blast and heat radiation from fuel-rich mixture detonation. *Shock Waves*, **6**, 1996, pp. 21-28.
17. https://publikationen.bibliothek.kit.edu/270060420